Electronic Supplementary Information

Hetero-epitaxial growth of vertically-aligned TiO_2 nanorods on m-cut sapphire substrate with (001) SnO_2 buffer layer

Won-Sik Kim, Yun-Guk Jang, Dai-Hong Kim, Hong-Chan Kim and Seong-Hyeon Hong*

Department of Materials Science and Engineering and Research Institute of Advanced Materials, Seoul National University, Seoul 151-744, Republic of Korea, Fax: +82-2-885 - 1748; Tel: +82-2-880-6273; E-mail: shhong@snu.ac.kr

1. Experimental Details

Preparation of SnO_2 buffer layer. M-cut (100) sapphire was used as a substrate. Before deposition, the substrate was ultrasonically cleaned in acetone, ethanol, and de-ionized water for 10 min. Highly (001) oriented epitaxial SnO_2 film was deposited by plasma enhanced atomic layer deposition (PE-ALD). The Sn precursor was dibutyl tin diacetate (DBTDA, $((CH_3CO_2)_2Sn[(CH_2)_3–CH_3]_2)$). The time sequence for source pulse, first purge, plasma pulse, and second purge was 2, 8, 10, and 8 s, respectively. The deposition was conducted with an rf power of 100W at 240 mTorr for 500 cycles. The SnO_2 buffered m-cut sapphire substrate was annealed at 600 ^oC to enhance their crystallinity before the TiO_2 nanorod growth.

Synthesis of TiO_2 nanorods. For TiO_2 nanorod growth, 25 mL of de-ionized water was mixed with 25 mL of concentrated hydrochloric acid (36.5% ~ 38% by weight) and stirred at ambient conditions for 5 min. and then 0.8 mL of titanium butoxide ($Ti(OBu)_4$, 97% Aldrich) was added to the solution and stirred until the solution became transparent. As-prepared solution was transferred to the Teflon-lined stainless steel autoclave with 120 mL capacity. A piece of SnO_2 buffered M-cut sapphire was placed against the wall of the Teflon-liner just below the solution surface. The hydrothermal synthesis was conducted at 150 °C for 0.5~3.0 h in an electric oven. After synthesis, the autoclave was naturally cooled to room temperature. The as-synthesised TiO_2 nanorods were taken out, rinsed with de-ionized water, and dried in ambient air.

Materials Characterization. The morphology of as-synthesized product was observed by field-emission scanning electron microscopy (FE-SEM, JSM-7401F, JEOL). The phase and in- and out of-plane orientation relationships between nanorods and substrate were examined by X-ray diffraction (XRD) and X-ray pole figure. The out-of plane orientation was examined by θ-2θ X-ray diffraction (Model D8-Advance, BRUKER MILLER Co.) using Cu Kα radiation (λ=1.5406Å), and the in-plane orientation was investigated by X-ray pole figure (Model X'Pert Pro, PANalytical, the Netherlands), which was performed in Schulz reflection geometry by

scanning the tilt angle of goniometer, χ (Chi), in the range of 0–85◦ and the azimuthal angle, ϕ (phi), in the range of 0–360◦ with a step size of 5◦. High-resolution transmission electron microscopy (HR-TEM, JEM-3000F, JEOL) analysis was further performed to investigate the crystal structure of nanorods and interfaces between nanorod, buffer layer, and substrate.

2. Results and Discussion

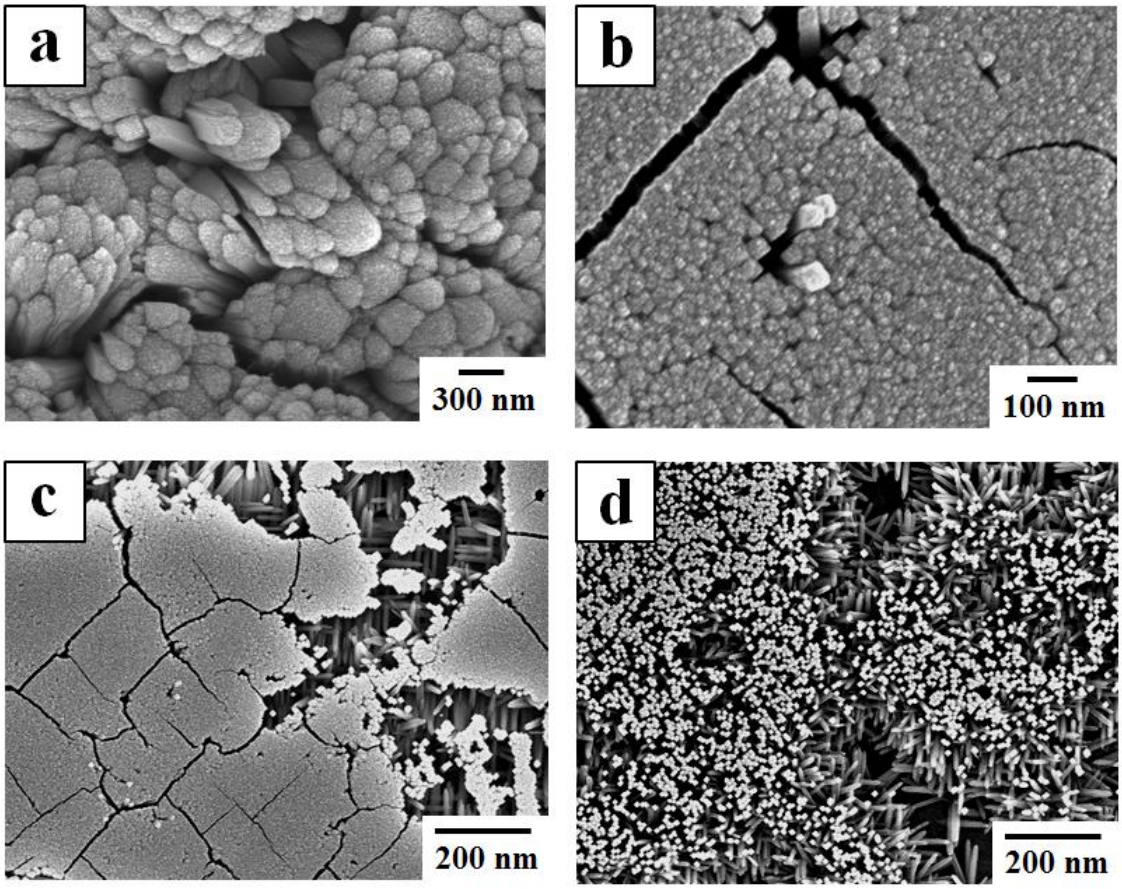

Figure S1. SEM images of TiO_2 rods grown on (a) bare m-cut sapphire and (b-d) SnO_2 buffered m-cut sapphire.

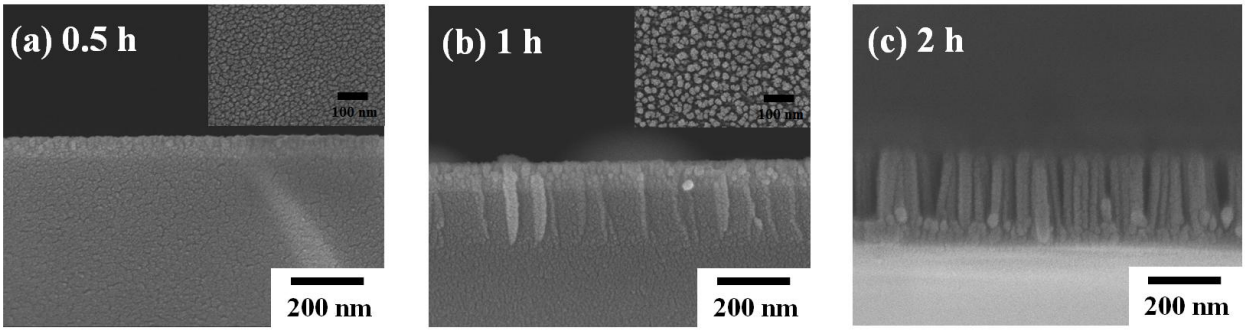

Figure S2. SEM images of TiO_2 rods grown for (a) 0.5 h, (b) 1.0 h, and (c) 2.0 h..

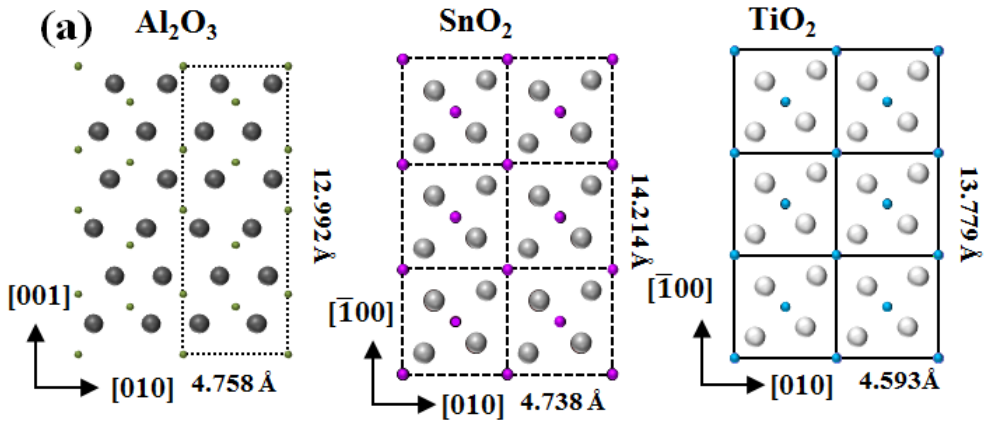

(b)

	Lattice mismatch	
SnO_2 / Al_2O_3	[010] / [010]	[1̄00] / [001]
	~ -0.42 %	~ 9.47 %
TiO_2 / SnO_2	[010] / [010]	[1̄00] / [1̄00]
	~ -3.06%	~ -3.06%

Figure S3. (a) Atomic configurations of m-cut sapphire, SnO_2 buffer layer, and TiO_2 nanorod based on the determined in-plane orientation relationships and (b) estimated lattice mismatches.

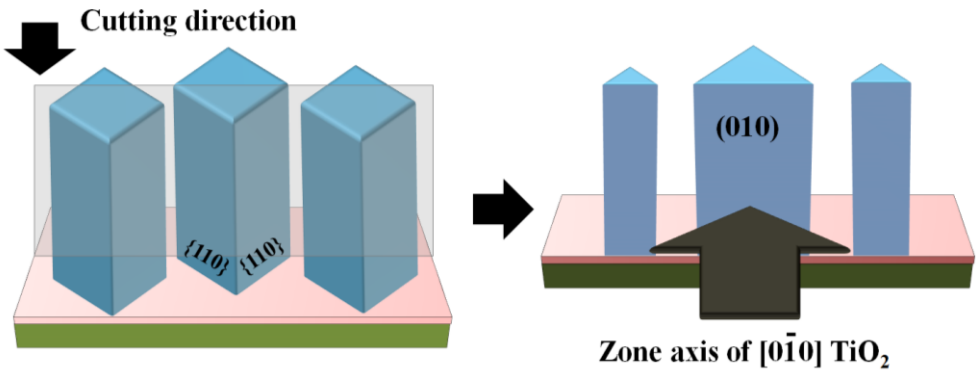

Figure S4. The preparation of cross-sectional TEM sample by FIB.

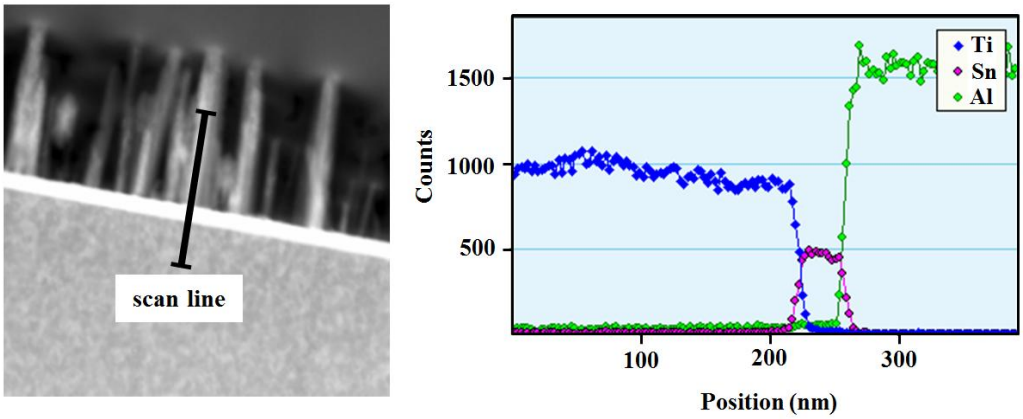

Figure S5. The energy dispersive X-ray spectroscopy (EDS) analysis of TiO_2 nanorods/SnO_2 buffer layer/m-cut sapphire substrate

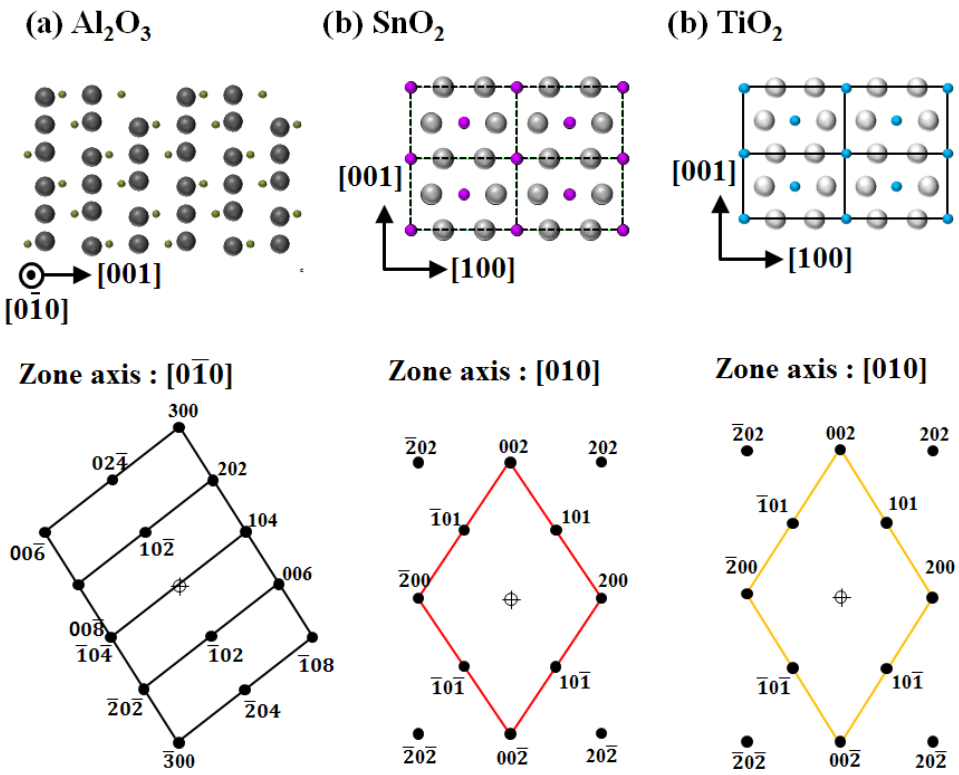

Figure S6. Atomic configurations and simulated diffraction patterns; (a) m-cut sapphire with a view direction of [0$\bar{1}$0], (b) SnO_2 buffer layer with a view direction of [010], and (c) TiO_2 nanorod with a view direction of [010].

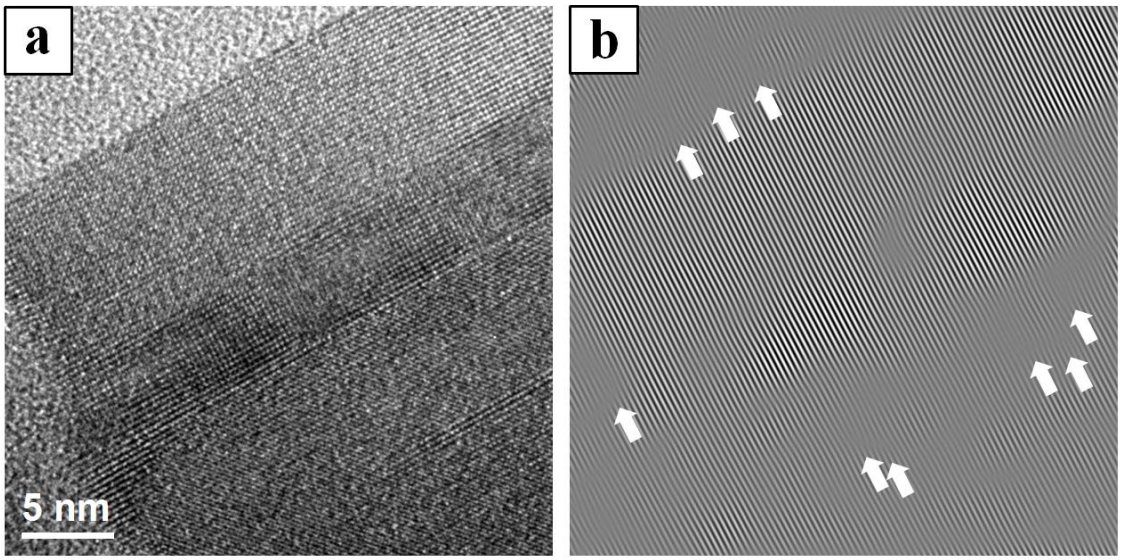

Figure S7. (a) HRTEM image of TiO_2 nanorod and (b) filtered FFT image of (a) (arrows indicate the line defects in the TiO_2 nanorods).

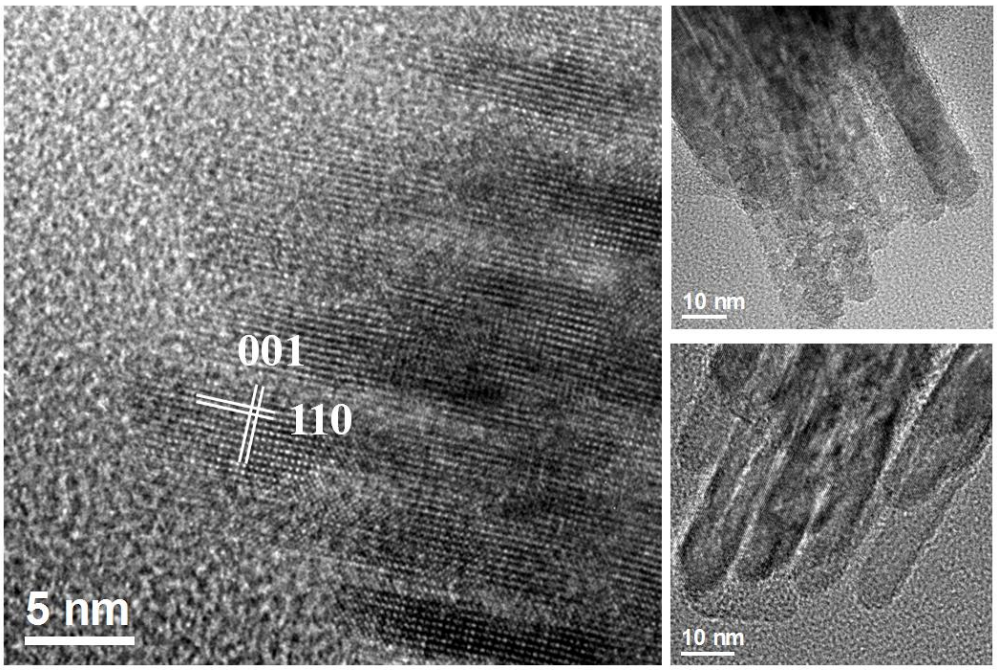

Figure S8. HRTEM images of TiO_2 nanorod tips.